On the Role of Nb on the Texture and Microstructure of a Novel As-rolled Medium Carbon Wear Resistant Slurry Pipeline Steel

Vahid Javaheri[1], Tun Tun Nyo[2], David Porter[3]

[1] Corresponding author, Ph.D. student, Department of Material Engineering and Production Technology, University of Oulu, Finland P.O. Box 4200, Tel: 00358-469341760, Email: Vahid.Javaheri@oulu.fi

[2] Research assistant, Department of Material Engineering and Production Technology, University of Oulu, Email: Tun.Nyo@oulu.fi

[3] Professor and Research Director, Department of Material Engineering and Production Technology, University of Oulu, Email: David.Porter@oulu.fi

Abstract:

A field emission scanning electron microscope equipped with EBSD has been employed to evaluate the role of 0.013 wt.% Nb on the evolution of the microstructure and texture of a novel thermomechanically processed low-alloy, medium-carbon steel. Specimens were subjected to hot-rolling with a total reduction of 80%, four passes in the recrystallization regime and four passes below the non-recrystallization temperature. Immediately after rolling, the strips were quenched to 420^{o}C and subsequently cooled slowly in a furnace to simulate strip coiling with transformation of austenite to bainite. The results showed that Nb microalloying results in a finer microstructure with a sharper texture when compared to an identical steel but without Nb. In addition, analysis of the retained austenite texture indicated that the main bcc texture components are the product transformed brass and copper components in the parent austenite.

Keywords: Hot deformation, Slurry pipe material, Texture, Microstructure, Niobium

1. *Introduction:*

Nowadays, the controlled rolling of steel pipe material has been widely used in the production of large diameter pipes for the oil and gas industry in order to improve the pipe performance by maximizing the grain refinement and achieve both higher strength and toughness in the steels [1,2]. Thermomechanical control process (TMCP) is a technological technique for improving the strength and toughness of steel plates by controlling the austenite microstructure via the rolling parameters and subsequent austenite transformation via control of the cooling path. Generally a multi-stage hot deformation process is applied with austenite deformation both above and below the non-recrystallization temperature (T_{NR}) [2,3]. During the rough rolling stage, deformation and repeated recrystallization above T_{NR} produces fine austenite grain structure which is elongated into a pancake shape after deformation below T_{NR}. The unrecrystallized austenite is then transformed to a fine microstructure the characteristics of which depend on the cooling pattern. Crystallographic texture develops in the austenite as a result of both recrystallization and deformation without recrystallization. Due to transformation orientation relationships the final ferritic microstructure also shows crystallographic texture [4]. When steel finish rolling is in the γ recrystallisation range, a weak transformation texture is produced in the α but with increasing amounts of deformation without recrystallization the texture of the ferrite becomes sharper [4].

Niobium (Nb) microalloying is often used to help control recrystallization, grain growth and phase transformations. It can also contribute to precipitation hardening of the final bcc microstructure [5,6].

The role of Nb in low-carbon steels has been thoroughly investigated [6–9]; however, the aim of the present study is to investigate the effect of a small addition of Nb on the microstructure and texture evolution during the thermomechanical controlled processing of a medium-carbon newly designed steel intended for wear resistant applications. The potential applications of this steel are still in the development phase but it mainly intended as slurry transportation pipe material.

2. *Experimental Material and Procedures:*

2.1. Material

The steel materials used in this work were produced in a vacuum-induction melting (VIM) furnace to ensure low impurity levels. Liquid metal was cast into a closed-bottom cast iron mould with internal dimensions: 51x310x600 mm. Nb was added to one of the samples. The steel chemical compositions are given in Table 1. The idea was to reduce the prior austenite grain size and widen the non-recrystallization region during hot rolling.

Table 1. Chemical composition of the samples (wt.%)

	C	Si	Mn	Cr	Ni	Mo	Nb	Al	N
Alloy 1	0.39	0.19	0.24	0.92	0.02	0.48	**0.002**	0.04	0.004
Alloy 2	0.39	0.18	0.24	0.92	0.02	0.58	**0.013**	0.04	0.004

2.2. Hot Rolling Process

As the thermomechanical controlled process, a slab-shape block (51x200x75 mm) of each casting was cut from the main cast block and reheated at 1200ºC for 3 hours. Then, they were rolled on a pilot rolling mill to a final thickness of 10 mm, Fig. 1a. Rolling was done in two stages: a 4-stage rough rolling (above the T_{NR} in the temperature range 1200-1100ºC with a total reduction of 48%) followed by a 4-pass finish rolling stage

below T_{NR} in the temperature range 950-800ºC with a total reduction of 62%. Subsequently, the rolled strips were directly quenched in water to 420ºC to achieve a microstructure comprising lower bainite. To simulate strip coiling, the strips were furnace cooled very slowly from 420°C, Fig. 1b. The temperature of the material during the whole of the above process was measured using a thermocouple inserted in the middle of the block before rolling.

2.3. Microtexture and Microstructure

Microstructural features were investigated using an optical and a laser scanning confocal microscope (VK-X200, Keyence Ltd.) after metallographic sample preparation and etching in 2 % Nital. A deep etching in a saturated aqueous picric acid solution with a few drops of detergent and hydrochloric acid was also utilized to reveal the parent austenite grain structure. A Sigma Zeiss field emission scanning electron microscope (FESEM) equipped by electron backscatter diffraction (EBSD) was employed for microtexture characterisation (working distance 15 mm and sample tilt 70º).

3. Results and Discussion:

3.1. Microstructure characterization

A combination of laser scanning and optical images showing a lath type of microstructure is presented in Fig. 2. In the sample containing Nb, the bainitic laths tended to nucleate and grow from the prior austenite grain boundaries, whereas without Nb, lath structure seems in no particular order. To identify the microstructural constituents of the specimen, EBSD analysis of lattice misorientations was applied based on the study of Zajac et al. [10].

The image quality, inverse pole figure map and misorientation angle distributions from 0° to 60° for the samples are shown in Fig. 3. It is observed that the relative frequency of high misorientation angles (more than 45°) is quite high in compared to the low angle misorientations (less than 15°). Zajac et al. [10] by analysing the misorientation angles of different types of bainitic microstructures, concluded that lower bainite is characterized by a misorientation spectrum with a high proportion of high-angle boundaries and relatively few low-angle boundaries exactly like those seen here. This indicates that direct quenching of the rolled strips to 420 °C led to austenite transformation to lower bainite.

3.2. Effect of Nb on the microstructure

It is widely reported [3,9,11–13] that trace amount of microalloying elements such as Nb can refine the microstructure and enhance the strength of low alloy steels during the production process from solidification to slab-reheating, controlled-rolling and accelerated cooling processes. The orientation of final as-cast structure and also of reconstructed prior austenite grain structure of the alloys and their hardness are given in Fig. 4.

In order to reveal the parent austenite grain structure, the EBSD data was subjected to a reconstruction technique using Matlab^{R} supplemented with the MTEX texture and crystallography analysis toolbox [14]. As the grain size was large, a series of 18 EBSD measurements were stitched merged together. Grain maps were initially assembled from the data sets with a grain boundary tolerance of 3 degrees. Subsequently, the parent austenite orientation map was reconstructed from this data with a two-step reconstruction algorithm. In the first step, the orientation relationship between austenite and martensite was determined from intergranular misorientations following the procedure proposed by Nyyssönen et al. [15]. In the second step, the grain map was divided into discrete clusters using the Markov clustering method [15] proposed by Gomes and Kestens [16]. The parent austenite orientation was then calculated for each cluster separately, resulting in a

reconstructed orientation map. The average misorientation between the reconstructed orientation for each cluster and the best fit for each individual grain was approximately 2 degrees, indicating a good fit for the reconstructed result. The full details for the reconstruction procedure are available in reference [17].

Although Nb was added due to its expected benefit during thermomechanical rolling, the results show that even during solidification Nb acts as a grain refiner and increases hardness, too.

Light optical images showing prior austenite structures are presented in Fig. 5. In both samples, there are some large elongated austenite grains that indicate that recrystallization did not take place completely in the rough rolling stage.

According to the thermodynamic calculation using Thermo-Calc software (Fig. 6), Nb should go completely into solid solution after reaching the slab reheating temperature, even in the interdendritic regions that have higher Nb contents. The solubility temperatures of niobium carbonitrides for both dendritic and interdendritic region are marked on the Fig. 6. The amount of Nb in the interdendritic region was calculated using segregation simulation. As rough rolling took place between 1200°C and 1100 °C, the Nb during this step should mostly be in solid solution since niobium carbonitrides (Nb(CN)) starts to form below 1110 °C.

Maruyama and Smith [6], by using a 3D atom probe, showed that the onset of recrystallization can be prevented by solute interstitial atoms and small substitutional-interstitial atomic clusters rather than by fine Nb precipitates. Fine Nb(CN) which precipitates during finish rolling can prevent dynamic recrystallization by inhibition of subgrain boundary movement and the dragging of crystalline defects such as ledges and deformation bands due to the lattice mismatch with austenite and even ferrite [12,13].

Fig. 7 (a, c) shows the crystal orientation map merged with the image quality of the bainitic structure along the rolling direction. Each colour indicates a specific crystal orientation, which the misorientation between two neighbours greater than 15° is defined as a high-angle grain boundary. The calculated average grain diameter was 19 and 35 μm for the sample containing Nb and without Nb, respectively. One example of the grain structure and grain size distribution of the bainitic structure of both alloys at a very high magnification is given in Fig. 8. The reconstructed parent austenite grain structure is also given in Fig. 7(b, d). It can be seen that the sample containing Nb has a finer prior austenite structure. The equiaxed grains and elongated grains are also seen due to incomplete recrystallization during hot-rolling.

Furthermore, Nb suppressed austenite grain growth during the slab reheating thanks to the pinning effect on the grain boundaries. Nb is expected to delay the early stage austenite recrystallization during the subsequent rough rolling process due to inhibiting subgrain boundaries movement by strain induced carbonitrides precipitated [11] or dragging the vacancies and dislocations by solute Nb atoms [9].

3.3. Macrotexture Investigation

Orientation distribution function (ODF) is a both powerful and frequently used mathematical technique to describe the frequency of occurrence of particular crystal orientations in a three-dimensional Euler orientation space. In BCC materials (like the material used in this work), the major texture components and fibers of rolled sheet (either in the deformed or annealed condition) can be found in the φ_2=45° section of Euler space [18]. Fig. 9 is a schematic illustration of the ideal position of these main components in the φ_2=45° section.

ODF maps of φ_2= 0° and φ_2= 45° of the samples are depicted in Fig. 10 and also volume fraction and distribution of each components in the microstructure are given in Fig. 11, as well. As expected, the ODF

sections show that the texture of the alloys was the typical texture of rolled carbon steel containing mainly ND (γ) and RD (α) fibers. It can be seen that the volume fractions of the main transformed components in the sample containing Nb was a little greater than in the sample without Nb. In general, the sharpness of the texture and the relative intensities of the various components depend on the composition of the steel, amount of reduction, initial austenite grain size, and cooling rate during transformation [4]; as all of these factors were similar for the both specimens it could be assumed that the sharpness in the texture of the Nb microalloyed sample might be due to one or two main reasons, decreasing the austenite grain size by Nb and the precipitation of NbC during rough rolling which suppresses the recrystallization of austenite that lead to austenite pancaking (transformation of unrecrystallized austenite) starts at higher temperature.

As can be seen in Fig. 11, the addition of Nb increased the strength of the {110}[001] (Rotated-cube) component. This is probably because Nb strengthens the cube component in the parent austenite as reported in the related reference [4]. Recrystallization occurs faster in fine-grained materials compared to the coarse-grained materials due to the increased grain boundary area providing more nucleation sites for recrystallization, which gives the sharper initial austenite cube component in the sample containing Nb.

Fig. 12 presents microtextural details of the samples including the α, γ and ε-fibers. On the α and γ-fiber the most important rolling components under plain strain deformation can be seen. The γ-fiber also comprises important recrystallisation components, especially close to {111} < 112> [19]. With regard to Fig. 10 (a), the orientation density of α-fiber in both samples are mainly located near (223)[110] and (112)[110]. Furthermore, the intensity of all orientations is almost the same for both samples. Regarding Fig. 10 (b), it is worth noting that there is almost no dominant orientation along the γ-fiber for either steel composition. However, relatively strong orientations can be seen at (111)[112] and (111)[123]. Fig. 10 (c) shows that the orientation density of ε-fibers is mainly centred on (332)[113] and (552)[225] which are transformed components originating from the parent austenite brass component. It has been reported by [4,20,21] that among the transformation texture components found in controlled rolled oil and gas pipeline steels that have low amount of carbon, the (113)[110] component causes significant anisotropy in mechanical properties i.e. both strength and toughness specially along the 45◦ plane with respect to the rolling direction. By contrast, less anisotropy in strength and toughness is reached when the (332)[113] component is strong. This indicates that the composition containing Nb may have better strength and toughness than that without Nb as the intensity of its (332)[113] component is 3 times higher than the steel without Nb.

Since the final room temperature microstructure contains a small fraction of retained austenite, it was possible to determine the texture of the austenite as a representative of the parent fcc phase before quenching and transforming to the bcc texture, as shown in Fig 13.

By comparing Fig. 10 and Fig. 13, it could be concluded that main transformation texture components (transformed and rotated brass, transformed copper, and rotated cube) originated from a pancaked austenite rolling texture, with the characteristic components of copper ({112}[111]), goss ({110}[001]), and brass ({110}[112]), which is schematically illustrated in the Fig. 14. This is to be expected since when austenite is rolled below the T_{NR} temperature, the deformation texture components are no longer removed by recrystallization.

4. Conclusions:

A FESEM equipped with EBSD has been employed to study the effect of 0.013 wt.% Nb on the microtexture and microstructure of a novel medium-carbon low-alloy wear resistant steel composition produced using thermomechanical controlled rolling and direct quenching to simulate strip rolling with coiling at 420°C. The following conclusions can be drawn:

- After controlled hot rolling of the medium-carbon low-alloy samples and direct quenching to the 420°C, a lath type lower bainitic microstructure was formed during $\gamma - \alpha$ transformation. The addition of 0.013 wt.% Nb refines the prior austenite and bainite structures and increases the hardness of the final microstructure.

- Refinement the prior austenite grain structure by Nb, caused a sharper texture of the sample containing Nb in compared to an identical steel but without Nb.

- The ODF of the alloys shows that the finish rolling temperature was low enough to sharpen this desired $\{332\}\langle 113\rangle$ texture component, which is expected to improve the both toughness and strength.

- Analysis of the retained austenite texture indicated that the main bcc texture components are the product transformed brass and copper components in the parent austenite.

-

5. Acknowledgements

The authors are grateful for financial support from the European Commission under grant number 675715 – MIMESIS – H2020-MSCA-ITN-2015, which is a part of the Marie Sklodowska-Curie Innovative Training Networks European Industrial Doctorate programme.

6. References:

[1] E. El-Danaf, M. Baig, A. Almajid, W. Alshalfan, M. Al-Mojil, S. Al-Shahrani, Mechanical, microstructure and texture characterization of API X65 steel, Mater. Des. 47 (2013) 529–538. doi:10.1016/j.matdes.2012.12.031.

[2] M. Eskandari, M.A. Mohtadi-Bonab, J.A. Szpunar, Evolution of the microstructure and texture of X70 pipeline steel during cold-rolling and annealing treatments, Mater. Des. 90 (2016) 618–627. doi:10.1016/j.matdes.2015.11.015.

[3] K. Nishioka, K. Ichikawa, Progress in thermomechanical control of steel plates and their commercialization, Sci. Technol. Adv. Mater. 13 (2012) 23001. doi:10.1088/1468-6996/13/2/023001.

[4] R.K. Ray, J.J. Jonas, M.P. Burton-Guillen, J. Savoie, Transformation textures in steels, ISIJ Int. 34 (1994) 972–942.

[5] L.J. Cuddy, grain refinment of Nb steels by control of recrystallization during hot rolling, Metall. Trans. A. 15A (1984) 87–98.

[6] N. Maruyama, G.D.W. Smith, Effect of nitrogen and carbon on the early stage of austenite recrystallisation in iron-niobium alloys, Mater. Sci. Eng. A. 327 (2002) 34–39. doi:10.1016/S0921-5093(01)01889-5.

[7] K.B. Kang, O. Kwon, W.B. Lee, C.G. Park, Effect of precipitation on the recrystallization behavior of a Nb containing steel, Scr. Mater. 36 (1997) 1303–1308. doi:10.1016/S1359-6462(96)00359-4.

[8] S.F. Medina, The influence of niobium on the static recrystallization of hot deformed austenite and on strain induced precipitation kinetics, Scr. Metall. Mater. 32 (1995) 43–48. doi:10.1016/S0956-716X(99)80009-0.

[9] N. Maruyama, R. Uemori, M. Sugiyama, The role of niobium in the retardation of the early stage of austenite recovery in hot-deformed steels, Mater. Sci. Eng. A. 250 (1998) 2–7. doi:10.1016/s0921-5093(98)00528-0.

[10] S. Zajac, V. Schwinn, K.H. Tacke, Characterisation and Quantification of Complex Bainitic Microstructures in High and Ultra-High Strength Linepipe Steels, Mater. Sci. Forum. 500–501 (2005) 387–394. doi:10.4028/www.scientific.net/MSF.500-501.387.

[11] I. Weiss, J.J. Jonas, Interaction between RecrystalIization and Precipitation Duringlhe High Temperature deformation of HSLA Steels\t, Metall. Trans. A. 10 (1979) 831–840.

file://ce/rd_organisation/PTA-MAD/Common/10 Literature/2008/Recov_Rex_GrainGrowth/Stat Rex/Weiss (1979) # Interaction between RecrystalIization and Precipitation Duringlhe High Temperature deformation of HSLA Steels.pdf.
[12] A.J. Deardo, Niobium in modern steels, Int. Mater. Rev. 48 (2003) 370–402.
[13] A.J. DeArdo, M.J. Hua, K.G. Cho, C.I. Garcia, On strength of microalloyed steels: an interpretive review, Mater. Sci. Technol. 25 (2009) 1074–1082. doi:10.1179/174328409X455233.
[14] T. Nyyssönen, M. Isakov, P. Peura, V.-T. Kuokkala, Iterative Determination of the Orientation Relationship Between Austenite and Martensite from a Large Amount of Grain Pair Misorientations, Metall. Mater. Trans. A. 47 (2016) 2587–2590. doi:10.1007/s11661-016-3462-2.
[15] S. van Dongen, Graph Clustering by Flow Simulation, University of Utrecht, 2000.
[16] E. Gomes, L.A.I. Kestens, Fully automated orientation relationship calculation and prior austenite reconstruction by random walk clustering, IOP Conf. Ser. Mater. Sci. Eng. 82 (2015) 12059. doi:10.1088/1757-899X/82/1/012059.
[17] T. Nyyssönen, Quenching and Partitioning of High-Aluminum Steels, Tampere University of Technology, 2017. https://tutcris.tut.fi/portal/files/9350586/nyyss_nen_1451.pdf.
[18] R.W. Revie, Oil and Gas Pipelines: Integrity and Safety Handbook, Wiley, 2015.
[19] D. Raabe, K. Lücke, Texture and microstructure of hot rolled steel, Scr. Metall. Mater. 26 (1992) 1221–1226. doi:10.1016/0956-716X(92)90567-X.
[20] M.S. Joo, D.W. Suh, J.H. Bae, N. Sanchez Mouriño, R. Petrov, L.A.I. Kestens, H.K.D.H. Bhadeshia, Experiments to separate the effect of texture on anisotropy of pipeline steel, Mater. Sci. Eng. A. 556 (2012) 601–606. doi:10.1016/j.msea.2012.07.033.
[21] S. Nafisi, M.A. Arafin, L. Collins, J. Szpunar, Texture and mechanical properties of API X100 steel manufactured under various thermomechanical cycles, Mater. Sci. Eng. A. 531 (2012) 2–11. doi:10.1016/j.msea.2011.09.072.

Figures:

Fig 1. *a) Schematic presentation of thermomechanical rolling procedure. b) Coiling simulation process plotted on TTT diagram of the sample calculated using JMatPro software.*

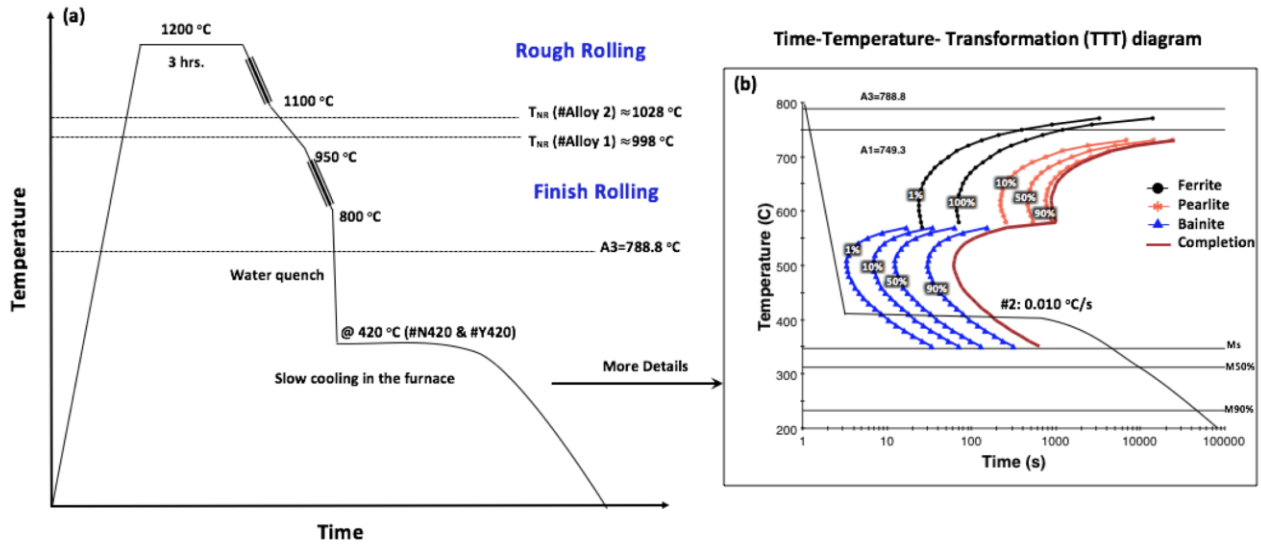

Fig 2. *As-rolled microstructures, a) sample containing Nb and b) sample without Nb (ND = strip normal direction, RD = rolling direction)*

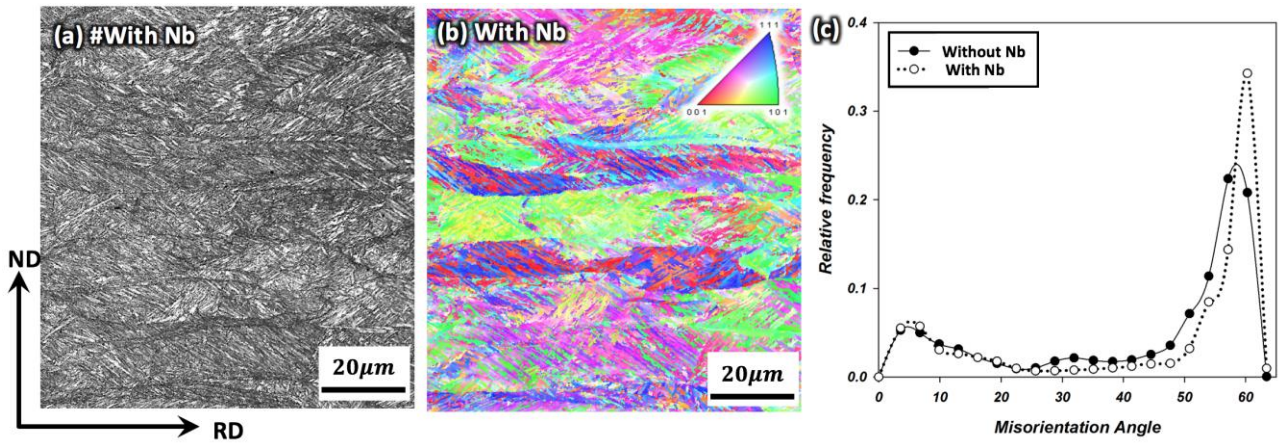

Fig 3. *a) Image quality of the sample containing Nb, b) inverse pole figure (crystallographic orientation map) of sample containing Nb, and c) misorientation angle distribution of both samples*

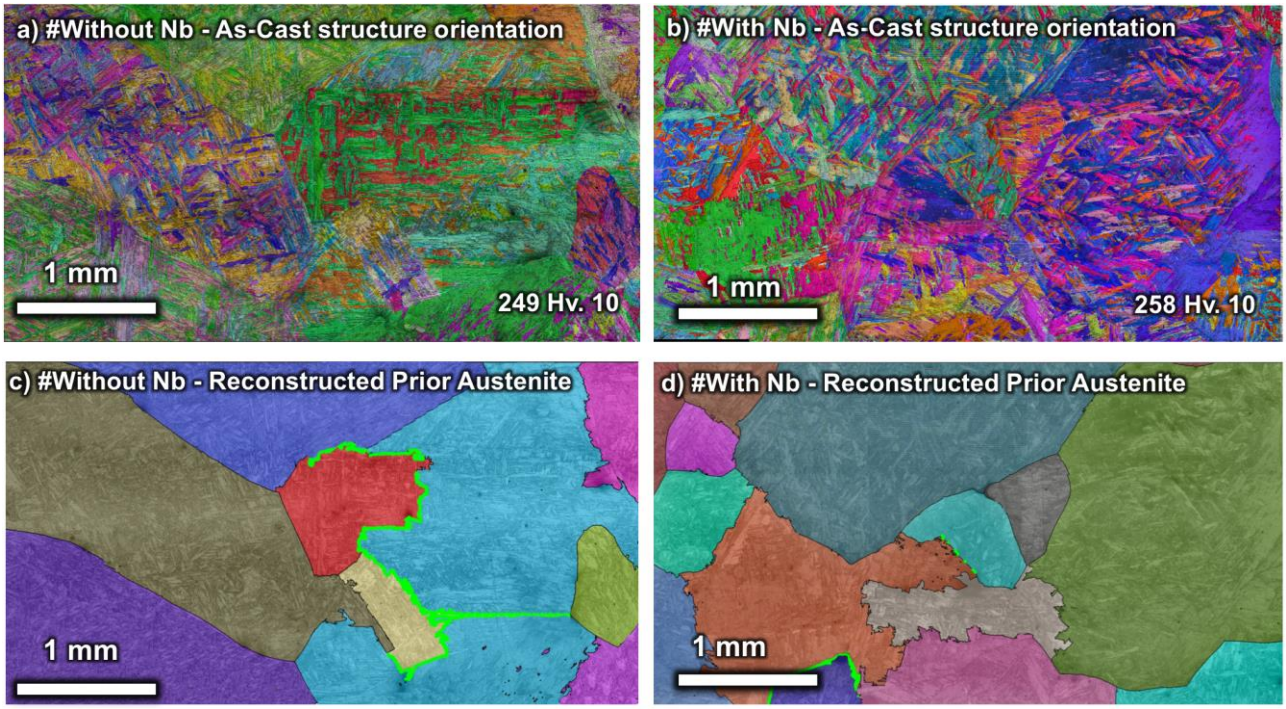

Fig 4. *a) and b) Crystallographic orientation maps of the as-cast materials including hardness values without and with Nb. c) and d) reconstructed parent austenite grain structure without and with Nb*

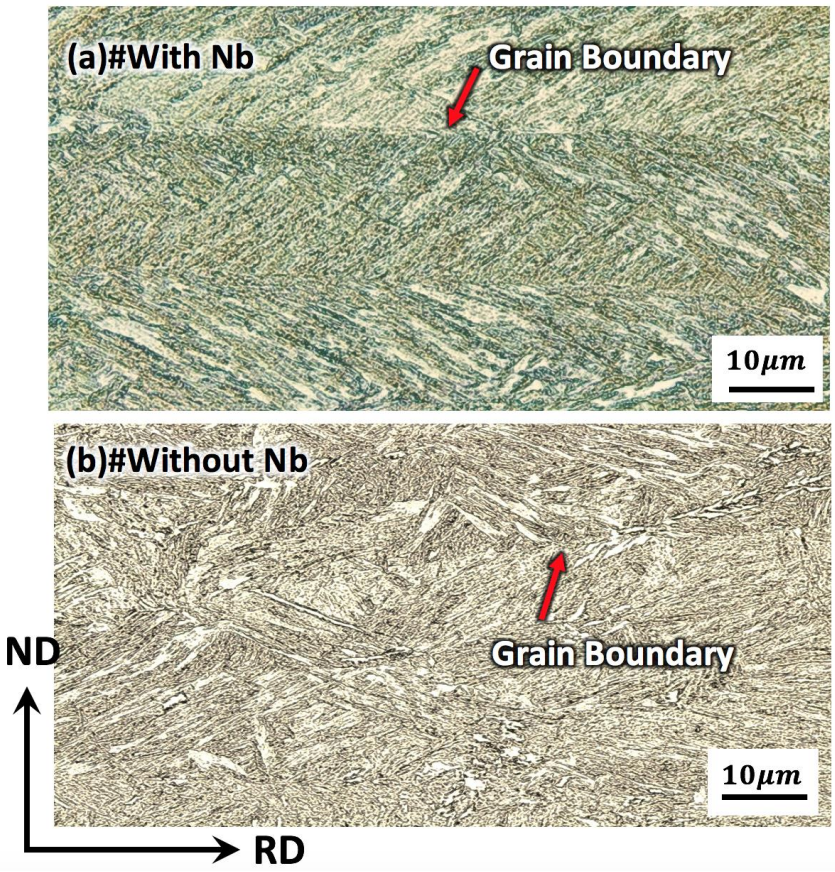

Fig 5. *Light optical microstructure of parent austenite a) without Nb and b) with Nb*

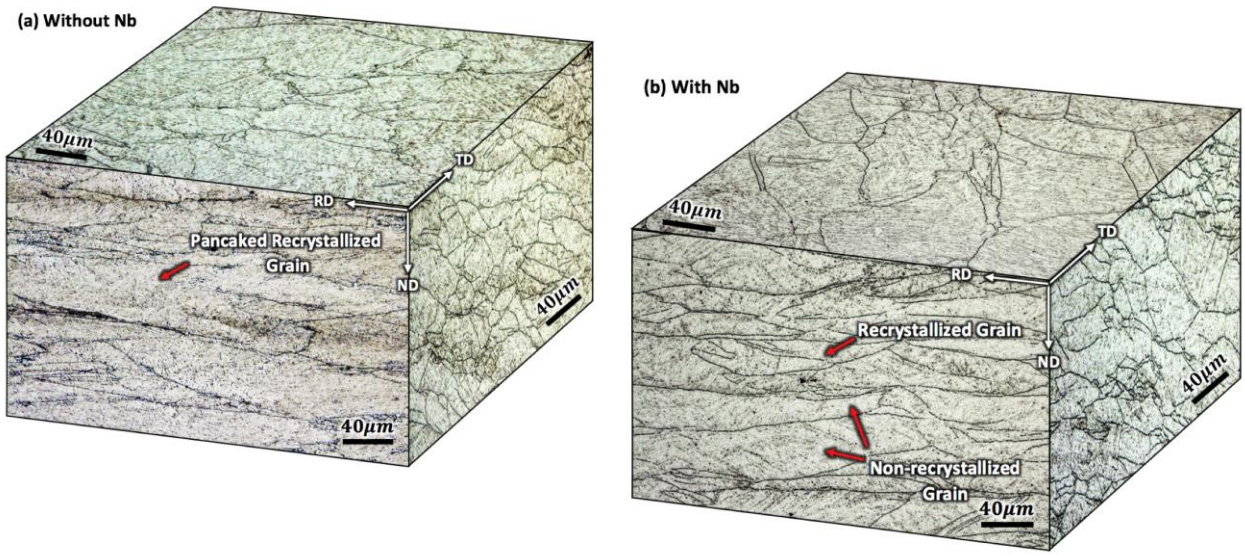

Fig 6. *Phase diagram showing the Nb solubility value for both amount of Nb in the dendritic and interdendritic region*

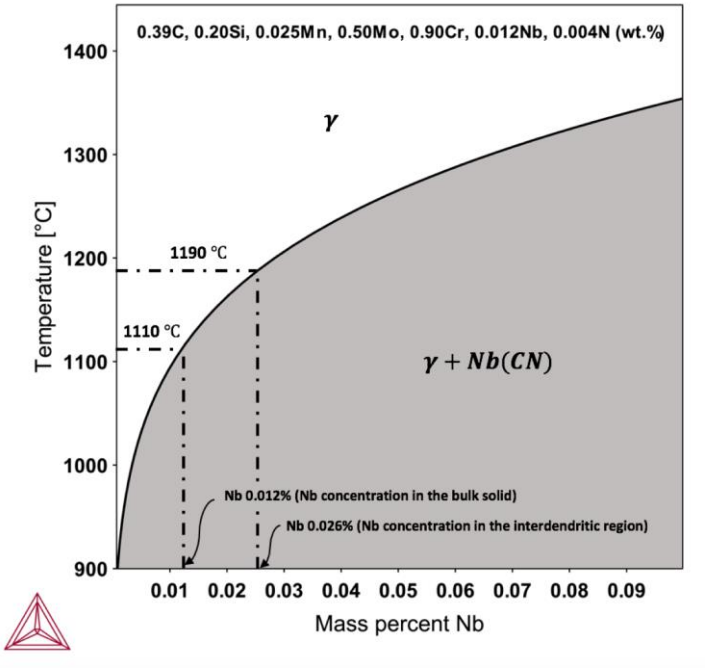

Fig 7. *Crystallographic orientation map and reconstructed parent austenite grain structure of sample. a, b) with Nb and c, d) without Nb*

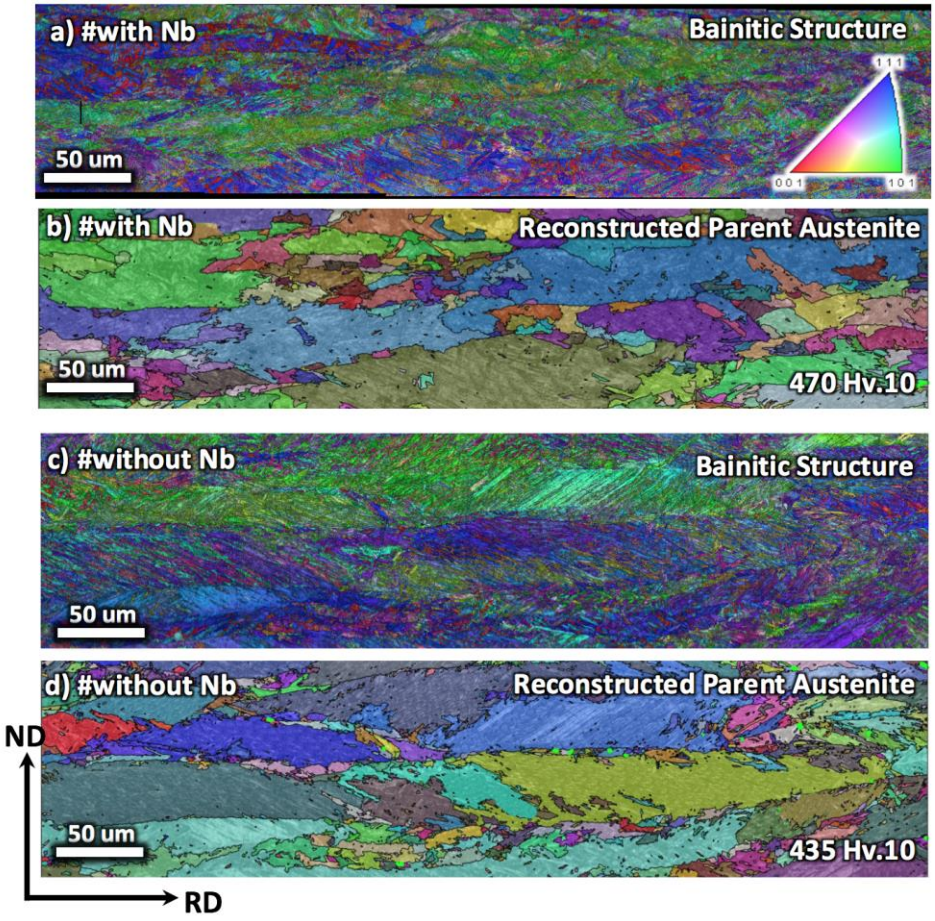

Fig 8. *Unique grains structure and their distribution of the sample a) with Nb and b) without Nb*

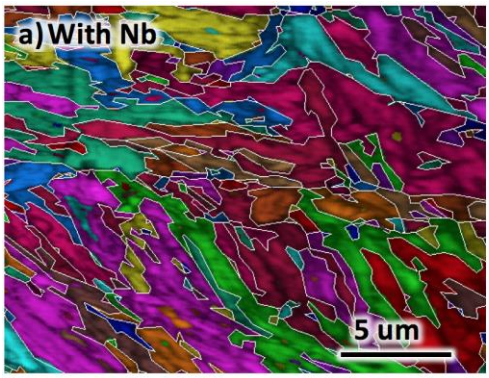

	Average Grain diameter range (μm)		Volume fraction
	Min	Max	%
1	0.127	5.598	60.3
2	5.598	7.916	23.7
3	7.916	9.694	9.70
4	9.694	11.194	0.00
5	11.194	12.515	6.40
6	12.515	15.364	0.00

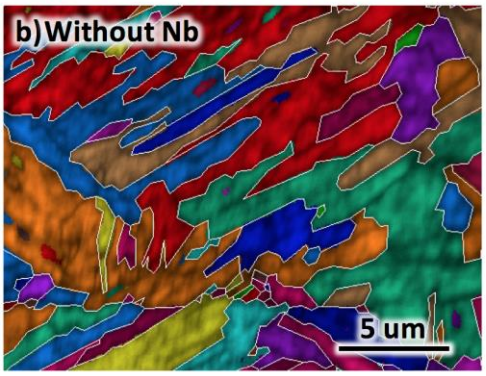

	Average Grain diameter range (μm)		Volume fraction
	Min	Max	%
1	0.127	5.598	56.0
2	6.273	8.871	18.2
3	8.871	10.864	4.90
4	10.864	12.545	0.00
5	12.545	14.026	8.60
6	14.026	15.364	0.00
7	15.364	16.595	12.2

Fig 9. *The important fibers and texture components of BCC steels in the φ_2=45° section of ODF*

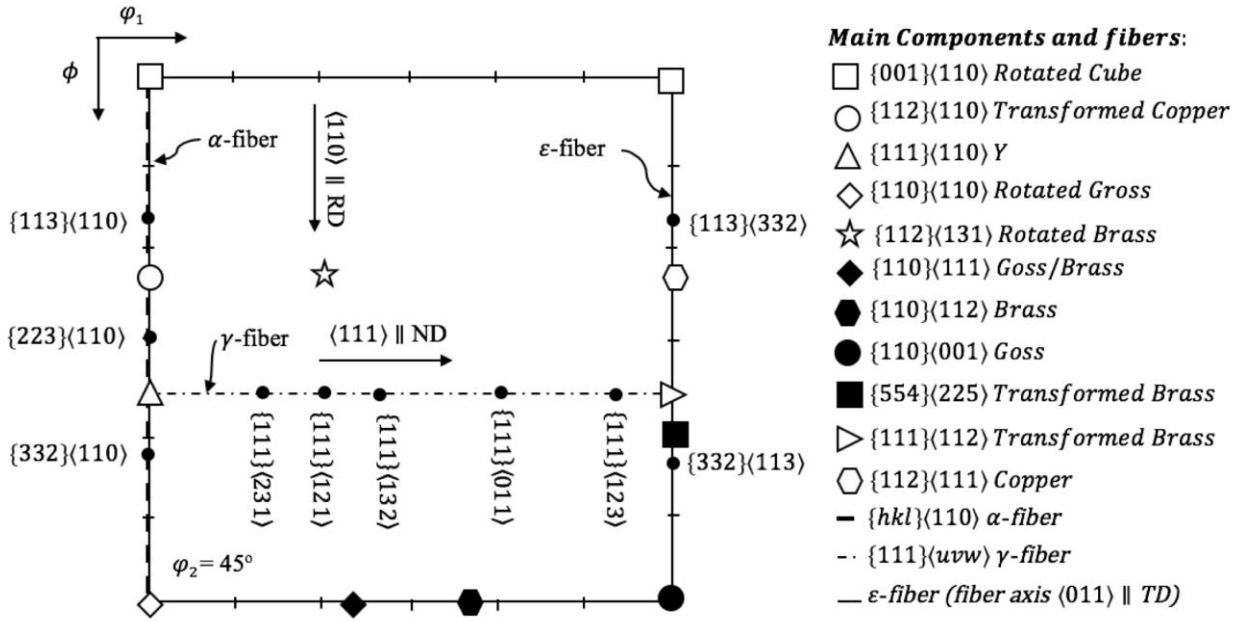

Fig 10. *The microtexture analysis of the sample, ODF phi$_2$= 0 and 45° of the sample a) without Nb and b)*

with Nb

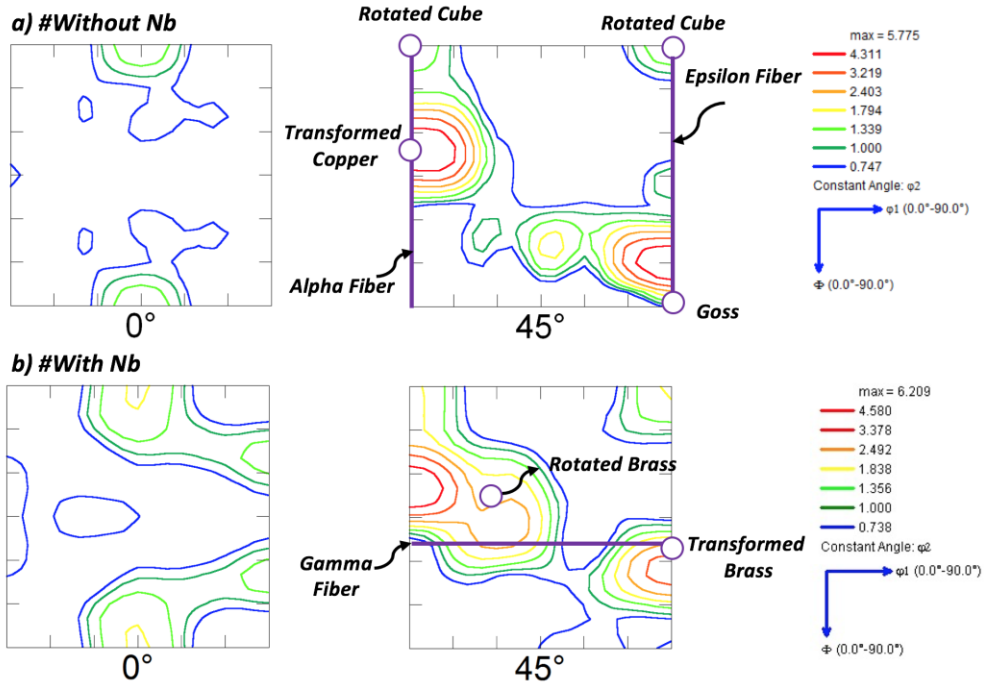

Fig 11. *Main crystal orientation components a) with Nb and b) without Nb. Volume fractions and more details in attached table*

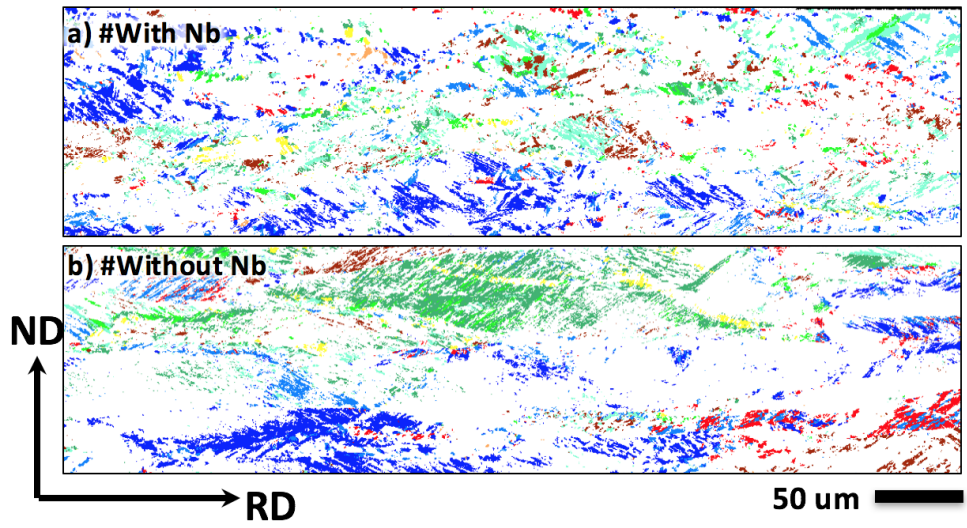

COMPONENT		EULER ANGLES, ° $(\varphi_1, \emptyset, \varphi_2)$	ORIENTATION	VOLUME FRACTION %	
				With Nb	Without Nb
	Transformed Cu	0, 35, 45	$(112)[1\bar{1}0]$	6.3	5.8
	Transformed Cu	0, 25, 45	$(113)[1\bar{1}0]$	3	2.5
	Rotated Cube	0, 0, 45	$(001)[1\bar{1}0]$	1.7	1
	Transformed Br	90, 54.74, 45	$(111)[\bar{1}\bar{1}2]$	2	1.4
	Cube	0, 0, 0	$(001)[100]$	0.2	0
	Goss	90, 90, 45	$(110)[001]$	0.4	0.5
	-	15, 47, 68	$(525)[1\bar{5}1]$	1.3	6.2
	-	23, 50, 56	$(323)[1\bar{3}1]$	3.9	1.3
	γ-Fiber component	60, 55, 45	$(111)[0\bar{1}1]$	0.9	1.6

Fig 12. *a) Rolling (Alpha), b) normal (Gamma), c) transverse (Epsilon) texture fibers, and d) schematic illustration of location of these fibers in Euler Space*

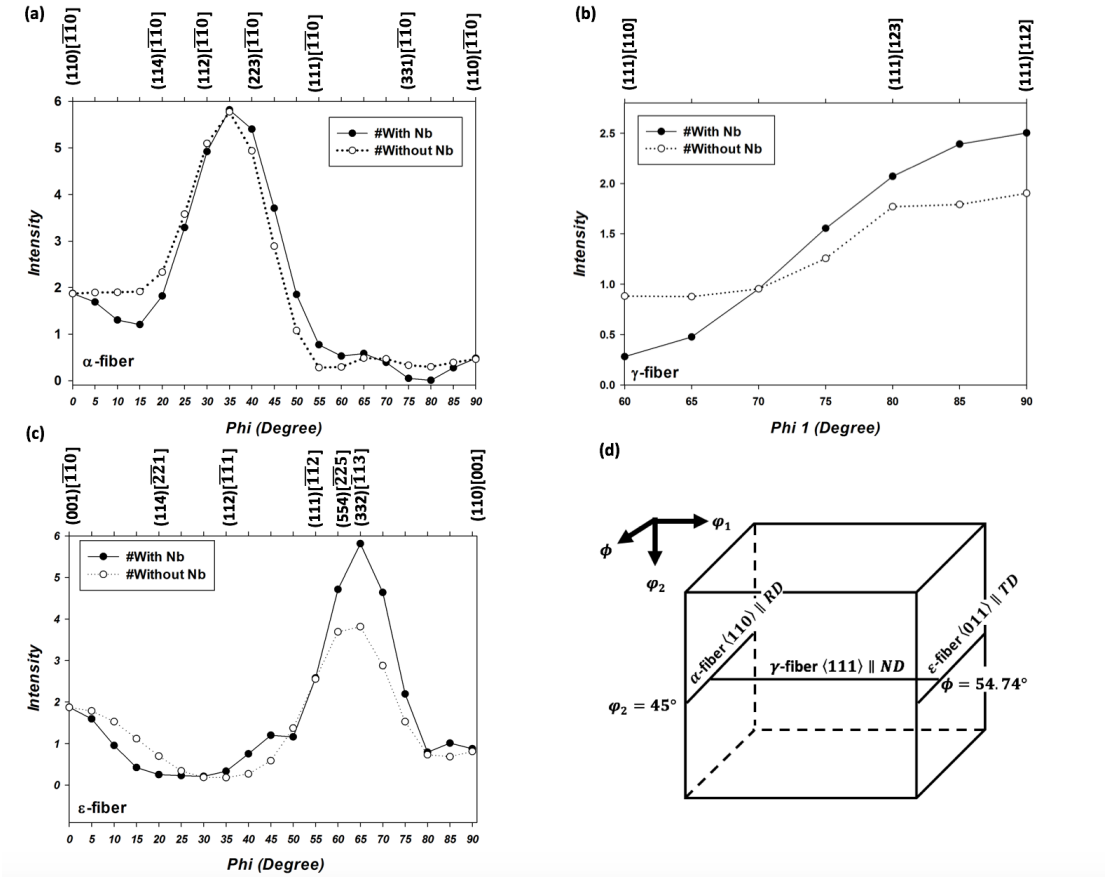

Fig 13. *Microtexure analysis of the retained austenite of the sample containing Nb, ODF phi₂=45°*

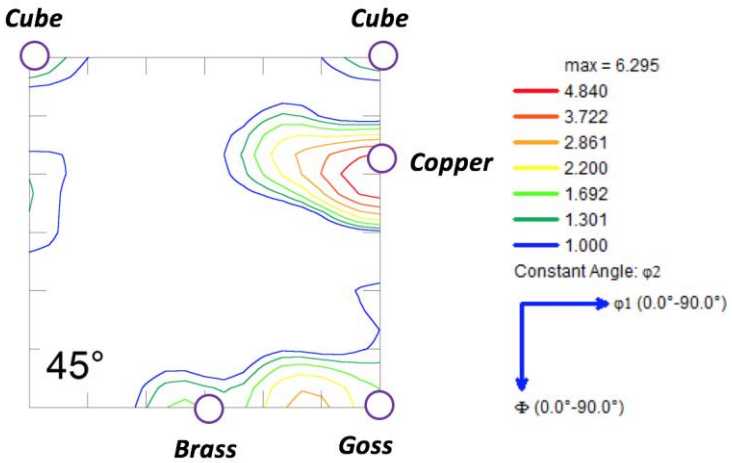

Fig 14. *Schematic illustration of the transformation of fcc rolled texture components to the bcc texture components during cooling and phase transformation*